metrology

MDPI

Article

Measurement Uncertainty Evaluation for Sensor Network Metrology

Peter Harris [1,*], Peter Friis Østergaard [2], Shahin Tabandeh [3], Henrik Söderblom [3], Gertjan Kok [4], Marcel van Dijk [4], Yuhui Luo [1], Jonathan Pearce [1], Declan Tucker [1], Anupam Prasad Vedurmudi [5] and Maitane Iturrate-Garcia [6]

1 National Physical Laboratory, Hampton Road, Middlesex, Teddington TW11 0LW, UK; yuhui.luo@npl.co.uk (Y.L.); jonathan.pearce@npl.co.uk (J.P.); declan.tucker@npl.co.uk (D.T.)
2 Danish Technological Institute, Kongsvang Allé 29, 8000 Aarhus, Denmark; peo@teknologisk.dk
3 VTT MIKES, Tekniikantie 1, 02150 Espoo, Finland; shahin.tabandeh@vtt.fi (S.T.); henrik.soderblom@vtt.fi (H.S.)
4 Van Swinden Laboratorium, Thijsseweg 11, 2629 JA Delft, The Netherlands; gkok@vsl.nl (G.K.); mvdijk@vsl.nl (M.v.D.)
5 Physikalisch-Technische Bundesanstalt, Abbestr. 2-12, 10587 Berlin, Germany; anupam.vedurmudi@ptb.de
6 Federal Institute of Metrology, Lindenweg 50, 3003 Bern-Wabern, Switzerland; maitane.iturrate@metas.ch
* Correspondence: peter.harris@npl.co.uk

Abstract: Sensor networks, which are increasingly being used in a broad range of applications, constitute a measurement paradigm involving ensembles of sensors measuring possibly different quantities at a discrete sample of spatial locations and temporal points outside the laboratory. If sensor networks are to be considered as true metrology systems and the measurement results derived from them used for decision-making, such as in a regulatory context, it is important that the results are accompanied by reliable statements of measurement uncertainty. This paper gives a preview of some of the work undertaken within the European-funded 'Fundamental principles of sensor network metrology (FunSNM)' project to address the challenges of measurement uncertainty evaluation in some real-world sensor network applications. The applications demonstrate that sensor networks possess features related to the nature of the measured quantities, to the nature of the measurement model, and to the nature of the measured data. These features make conventional methods of measurement uncertainty evaluation, and established guidelines for measurement uncertainty evaluation difficult to apply. An overview of some of the modelling tools used to address the challenges of measurement uncertainty evaluation in those applications is given.

Keywords: sensor network; measurement uncertainty; Kalman filter; Laplace transform; Gaussian process model; inverse problem

Academic Editor: Simona Salicone

Received: 19 September 2024
Revised: 30 October 2024
Accepted: 30 December 2024
Published: 9 January 2025

Citation: Harris, P.; Østergaard, P.F.; Tabandeh, S.; Söderblom, H.; Kok, G.; van Dijk, M.; Luo, Y.; Pearce, J.; Tucker, D.; Vedurmudi, A.P.; et al. Measurement Uncertainty Evaluation for Sensor Network Metrology. *Metrology* **2025**, *5*, 3. https://doi.org/10.3390/metrology5010003

1. Introduction

The conventional paradigm in metrology focusses on the measurement of a single, well-understood quantity, such as the amount of substance fraction of a certain gas compound in a gas mixture. For that purpose, a single, well-characterised (i.e., calibrated) measuring system or instrument operating in controlled, laboratory conditions is used. In this paradigm, the concepts of measurement uncertainty, calibration, metrological traceability [1] and traceability to the SI [2,3] are well-established and widely applied. These concepts are fundamental to ensuring that the quality of a measured value can be quantified, and that measurement results, for example, made at different times using different measuring instruments, can be compared. In recent times, however, there has been a rapid

uptake in the use of sensor networks (see [4] and the references therein), which constitute a different metrology paradigm. Here, a sensor network involves an ensemble of instruments measuring possibly different quantities at a discrete sample of spatial locations and temporal points outside the laboratory. Several aspects of the paradigm shift are highlighted in the following paragraphs.

Sensor networks have been deployed in a broad range of applications, which include in smart cities as part of smart energy grids [5,6], district heating systems [7,8] and air pollution monitoring systems [9,10], for environmental and climate monitoring [11–17], and in advanced manufacturing for condition monitoring and to support the 'Factory of the Future' [18–20]. The data provided by the sensor network are often used to make inferences about derived quantities at spatial locations and temporal points other than those at which measurements are made. Alternatively, data are aggregated [21,22] over a spatial region or time-period in order to decide, for example, whether a quantity of interest conforms to a regulatory requirement or to evaluate a spatial or temporal trend in the quantity.

The quality of the data, and of the information and decisions derived from the data, depend on how well the sensor network is designed and how the sensor data are analysed. For most applications, decisions are made based on the aggregation of sensor data gathered in situ (i.e., when deployed outside the laboratory). However, current practice in metrology [23] treats the sensors in a network as individual measuring instruments, meaning that calibration strategies are defined without reference to other sensors. Moreover, these calibration strategies depend in most cases on the comparison of sensor signals against the response of reference instruments performed under laboratory conditions [24–26]. Measurements made in controlled laboratory environments are important as a means to understand the cross-influence of sensors in a network and to eliminate possible deviations or influences from other variables, such as environmental variables. However, the in-situ behaviour and performance of the sensors in a network can be different from that under laboratory conditions where they are calibrated and tested. For example, their performance can drift, and they can fail when deployed in real-world environments under conditions they did not encounter during laboratory calibration, thus posing new metrological challenges. Such differences in behaviour are particularly evident when sensors are deployed in harsh or aggressive environments, such as the deployment of temperature sensors in factory environments where the sensors are subject to high temperature variations and high levels of dust, etc.

Measurement problems involving sensor networks have requirements and features that make the application of conventional methods of measurement uncertainty evaluation, and the use of established guidelines for measurement uncertainty evaluation, challenging. These requirements and features relate (a) to the nature of the measured quantities, which can be functions of spatial location and time, (b) to the nature of the measurement model, which has to capture complex behaviour and can itself be uncertain, and (c) to the nature of the measured data, which can be large-scale and heterogenous. Such requirements and features can vary appreciably between sensor network applications, which means that application-specific methods are sometimes needed. Furthermore, if the sensor network is to be considered as a true metrology system, it is necessary that the results are accompanied by reliable statements of measurement uncertainty. This is particularly important if the measurement results derived from the network are to be used for decision-making, such as in a regulatory context. For that purpose, conventional methods of data analysis and measurement uncertainty evaluation need adaption and extension for sensor networks.

The European Partnership on Metrology [27] is funding the project 'Fundamental principles of sensor network metrology (FunSNM)' [28] to address some of the metrological challenges associated with the deployment of sensor networks in real-world applications.

One objective of the project is to develop reliable methods for the evaluation of measurement uncertainty that quantifies one important aspect of the quality of the measured values obtained from the analysis of sensor network data. The project will build on previous work in the area, including [29–34]. The methods for measurement uncertainty evaluation should cover, for example, the proper treatment of correlation between the values recorded by individual sensors as well as sensor fusion that is 'uncertainty-aware' to account for heterogeneity in the sensors. Additionally, to ensure the trustworthiness of the measured values in a more general sense, the project aims to produce guidance on quality metrics for sensor networks and sensor network data that include not only measurement uncertainty but other descriptors, such as consistency, completeness, auditability, integrity, timeliness, uniqueness, and cost. The project will demonstrate the methods in the context of sensor networks deployed in different real-world applications covering networks of temperature sensors for district heating and for heat treatment of high-value engineering components, gas flow meter networks for natural gas and hydrogen distribution, air quality monitoring networks, and cost-efficient sensor networks combining hardware and soft sensors in smart buildings.

The focus of this paper is the topic of measurement uncertainty evaluation for sensor network metrology, and the aim of the paper is to give a preview of some of the work undertaken within the 'FunSNM' project on this topic illustrated by the real-world applications considered. In Section 2 the framework for measurement uncertainty evaluation that is commonly and successfully applied within the conventional paradigm of metrology is revisited, and reasons as to why that framework requires adaption and extension to meet the challenges from sensor networks are given. In Section 3 some examples taken from the 'FunSNM' project of that adaption and extension, motivated by real-world applications, are described. Finally, Section 4 contains a summary and conclusions.

2. Conventional Methods of Measurement Uncertainty Evaluation in Metrology

The 'Guide to the expression of uncertainty in measurement (GUM)' [35] provides a framework for evaluating and expressing measurement uncertainty that is widely applied within the conventional paradigm of metrology. The basis of the framework is the use of a measurement model in the explicit form $Y = f(X_1, \ldots, X_N)$ to relate the univariate (or scalar-valued) quantity Y intended to be measured (i.e., the measurand) to a set of input or influence quantities $X_1, \ldots, X_N$ that describe sources of uncertainty in knowing the value of Y. The framework is founded on probability theory with knowledge about the X_i encoded by probability distributions. Those probability distributions together with the measurement model are used to infer the probability distribution for Y, which in turn encodes knowledge about the measurand. An important principle of the framework is that when combining quantitatively different sources of uncertainty those sources are treated the same, irrespective of the nature of the knowledge about the sources. For example, uncertainty sources will be treated equally whether the knowledge is obtained from a statistical analysis of repeated measured values or based on other information, such as prior knowledge or a previous measurement uncertainty evaluation.

The GUM suite of documents, comprising the GUM and accompanying supplements and supporting documents, describes a number of methods to implement the framework. One of these methods relies on the so-called 'law of propagation of uncertainty (LPU)'. In the LPU method, the probability distributions for the input quantities are summarized by their expectations, standard deviations and covariances (in the case of joint distributions), and degrees of freedom where appropriate. This information is then propagated through a linearization of the measurement model by means of the LPU and the Welch–Satterthwaite

formula [36,37] to obtain summary information about the measurand in the form of an estimate, standard uncertainty, and effective degrees of freedom. A Gaussian distribution (or a scaled and shifted Student's t-distribution) is used to characterize the measurand in order to obtain a coverage interval containing values of the measurand with a specified coverage probability, for example, 0.95 or 0.99.

The LPU method makes an assumption about the nature of the measurement model, namely that a linear Taylor expansion evaluated at the estimates of the input quantities provides an adequate representation of that model. It also makes an assumption about the nature of the distribution for the measurand, namely that a Gaussian distribution (or a scaled and shifted t-distribution) is an adequate representation of that distribution. A numerical approach, the Monte Carlo method (MCM) for the propagation of distributions, is also described [38] to address those cases when the assumptions of the LPU method do not apply [39]. Rather than a linear approximation to the model and summaries of the probability distributions for the input quantities, the MCM uses the measurement model and the probability distributions themselves. For that purpose, the MCM makes random draws $\xi_{1,r}, \ldots, \xi_{N,r}$ from the probability distributions for the input quantities $X_1, \ldots, X_N$, and uses the measurement model to evaluate possible values $\eta_r = f(\xi_{1,r}, \ldots, \xi_{N,r})$ of Y. The values η_r provide an approximation to the probability distribution for Y in terms of which information about the measurand, in the form of an estimate (expectation), standard uncertainty (standard deviation) and coverage interval, is evaluated. A disadvantage of the method is that it can be computationally expensive, particularly when the number of input quantities and/or the number of random draws is large, and the measurement model is costly to evaluate, although other sampling methods can be used to address that limitation [40].

The methods described in the GUM suite of documents also extend to measurands that are multivariate (or vector-valued) comprising quantities $Y_1, \ldots, Y_m$, and to measurement models that are implicit and take the generic form $h(Y; X_1, \ldots, X_N) = 0$ in the univariate case or $h(Y_1, \ldots, Y_m; X_1, \ldots X_N) = 0$ in the multivariate case [41].

However, there are a number of features of sensor networks and sensor network data that provide challenges to the use of the above framework within the paradigm of sensor network metrology. These features relate to the nature of the quantities involved including the measurand, to the nature of the measurement model, or to the nature of the measured data. The features are not restricted to sensor networks but common in applications where sensors networks are used.

The measurand can be a function of spatial location (x, y, z) and possibly time t and frequency ν (or wavelength λ). In this case, the measurand is described by a mathematical function denoted, for example, by $Y = f(x, y, z, t, \nu)$ rather than modelled as a scalar or vector-valued random variable. Even when the measurand of primary interest is itself scalar- or vector-valued, it will often be derived from an underlying function of that form, for example, by evaluating or integrating the function. This form of measurand, which is not treated within the GUM framework, poses challenges in the way that measurement uncertainty is evaluated and represented. Furthermore, the GUM framework only considers continuous quantities, but a sensor may record a quantity that is categorical (e.g., identifying only whether a stimulus such as an electric current is applied or not). Similarly, the measurand itself can be categorical, for example, a label denoting the presence or absence of a chemical compound at a specific location and time.

The measurement challenges in many emergent areas related to climate science, environmental monitoring and energy involve measurements made outside laboratory conditions where the responses of sensors have been carefully validated by well-established methods ensuring measurement traceability. In such cases, measurement models need to be

modified to accommodate the behaviour of the sensors in situ, and this behaviour may not be fully understood. The underlying physical system and, consequently, the measurement model representing that system, may be only partially known. Thereby, model uncertainty becomes an important source of uncertainty, which is not treated within the GUM framework. The measurement model may be physics-based (for example, in the form of partial differential equations), data-driven (for example, in the form of a deep neural network) or a mixture of the two. Furthermore, the measurement model may be 'dynamic' in the sense that sensors are used in circumstances in which the interaction between the sensor and the quantity it measures, which acts as a stimulus, is frequency dependent. Deconvolution methods are needed in this case to recover an estimate of the quantity from the recorded signal [42–44]. Moreover, many data analysis and modelling problems take the form of a regression or inverse problem, which are also not treated in the GUM framework.

Generally, the measured data from a sensor network is in the form of multiple time series. However, quite often, these time series are collected with different sampling frequencies, which requires timestamps and time synchronization [45], and can be subject to jitter [46], as well as information about the spatial locations of the sensors within a common frame of reference. Properties of sensor networks related to network size (the number of sensors) and operating duration among others lead to challenges around the management of large datasets and demands on the scalability of conventional approaches to measurement uncertainty evaluation [47]. The nature of the sensors will also influence the choice of approach or methodology: sensors can be homogeneous or heterogeneous, both in terms of the physical quantity they measure and in terms of their quality as expressed in terms of their measurement uncertainty, they can be subject to drift or not, they can become faulty and their performance can experience a step change after maintenance or re-calibration, they can provide observations that are uncorrelated or correlated, they can be stationary or moving, etc. All such features provide challenges to the way sensor network data are analysed and how measurement uncertainty is evaluated.

3. Examples from the FunSNM Project

In the following sub-sections, some examples of the sensor network problems treated in the 'FunSNM' project [28] are briefly described. The modelling tools used to address those problems, together with the implications for the treatment of measurement uncertainty, are indicated. Further details are available in published papers or those in preparation.

3.1. Model-Based Tree-Structured Mesh Networks

A relatively simple type of sensor network, often seen in utility networks in urban areas, is a tree-structured mesh network, used for distributing water, district heating, electricity, and town gas. Originally, these networks were rooted in a single production or supply facility, distributing the resources through a series of pipes, splitting into increasingly smaller branches at discrete points until arriving at the location of the consumer. Due to their simplicity, these networks have a number of advantages, making them easy to model, to estimate states of the system, and to propagate measurement uncertainty. As an example, a district heating network is considered, as illustrated in Figure 1.

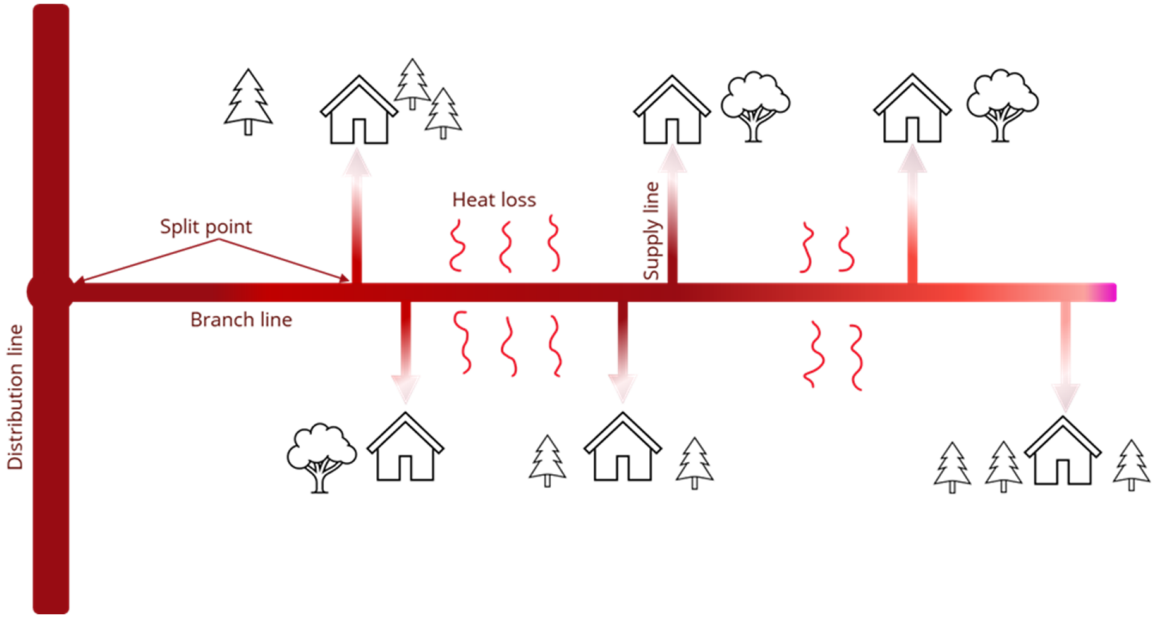

Figure 1. Small branch of a district heating network. Warm water enters from the left and is distributed to the connected houses. The district heating water continuously cools down as it gets further away from the heat plant.

District heating networks, with their tree structured topology, can be split into small segments, each starting and ending at a split point. For each of these segments, the system is practically one-dimensional with constant flow and, given a sufficient flow and uniform insulation of the pipe, its thermal behaviour is straightforwardly modelled. The loss of thermal energy $\dot{Q}$ (in W) in a segment of the pipe can be expressed as a function of the drop in temperature from one end of the pipe to the other:

$$\dot{Q} = c_{H_2O} \cdot q \cdot (T_M - T_C), \tag{1}$$

and obtained from the temperature difference between the water in the pipe and the ambient temperature:

$$\dot{Q} = U \cdot L \cdot \left(\frac{T_M + T_C}{2} - T_A \right). \tag{2}$$

In expressions (1) and (2), the following nomenclature is used: c_{H_2O} for volumetric heat capacity of water (in $\mathrm{Jm^{-3}K^{-1}}$), q for the water flow in the pipe (in $\mathrm{m^3s^{-1}}$), U for the insulation value of the service pipe (in $\mathrm{Wm^{-1}K^{-1}}$), L for the length of the service pipe (in m), T_M for the temperature at the start of the service pipe or main pipe (in °C), T_C for the temperature at the end of the service pipe at utility meter (in °C), and T_A for the ambient or ground temperature (in °C). The parameters q, L and T_C are known from the utility meters and geographic information system (GIS) data, while T_A is available from meteorological services. Combining the expressions (1) and (2) makes it possible to model the temperature at the main pipe (3) when knowing the length of the service pipe, the temperature of the ground, as well as the flow and the temperature at the utility meter:

$$T_M = T_C \frac{q + B}{q - B} - T_A \frac{2 \cdot B}{q - B}, \qquad \text{with} \qquad B = \frac{U \cdot L}{2 \cdot c_{H_2O}}. \tag{3}$$

In a network where utility meters measure temperature and flow at the terminal nodes or "leaves" of the tree-structured system, it is possible, by using expression (3), to find the temperatures at the main branches of the system. As the insulation values U of the service

pipes are not known exactly, and offset errors in the measurements of T_C can be present, the calculated values of T_M will also contain offset errors. The offset of T_M can be corrected for at the main pipe by performing a least-squares fit to a series of calculated T_M values (one for each service pipe) using the physical model given in (3) along with the known flow in each segment of the main pipe. Potentially, a circulation valve at the end of the main pipe must also be considered, adding a fixed flow to the system.

The procedure described above makes it possible to find the most probable temperature profile in the main branch of the utility. Transforming the temperature at the beginning of a service pipe back to an expected temperature at the utility meter of a consumer will give an offset to the utility meter. However, this offset can be caused both by an actual deviation in the utility meter, and from an offset in the expected insulation level of the service pipe. To estimate offsets in the utility meters, it is required to simultaneously find appropriate U-values for the service pipes. As such, the following system state vector is to be determined for a branch in the utility network:

$$\boldsymbol{x} = \begin{bmatrix} \delta T_1 & U_1 & \delta T_2 & U_2 & \cdots & \delta T_n & U_n \end{bmatrix}^{\mathrm{T}}, \tag{4}$$

where $\delta T_1, \delta T_2, \ldots \delta T_n$ are offsets to the temperature measured by the utility meter and $U_1, U_2, \ldots, U_n$ are the insulation values of the service pipes. Although the parameters in the system state vector appear to be independent, incorrect estimates of them will influence the calculated value in the main branch, and thereby the calculated offset of the other meters, by which a correlation between the elements will arise. This correlation can be utilized when identifying the values.

A widely used method for estimating the state of a system is the Kalman filter [48]. The standard Kalman filter requires that the system is linear, which is not the case for district heating, as the heat loss given by expression (3) is highly nonlinear with regards to both the flow in the pipes and the U-value of the service pipe. Modifications of the Kalman filter exist for non-linear systems, most notably the 'Extended Kalman Filter' (EKF) [49] and the 'Unscented Kalman Filter' (UKF) [50]. The UKF has the advantage that the model given in expression (3) can be used directly without the need for linearization.

Kalman filters have the advantage that they work with probability distributions. Because of this, the uncertainty of the estimate of the state can be calculated along with the value of the estimate. When more measurements are performed then both the estimate of the state and its uncertainty are updated. The calculated uncertainty for the meter offset found using the Kalman filter depends both on the noise and reproducibility of the meter, as well as on the models used to transform the temperatures between T_C and T_M in the Kalman filter.

The UKF has many advantages when used to estimate the state of a utility network. It can harness the knowledge of the physical system and use it to decrease the uncertainty of the measurements, it can use the data from nearby meters to give a better estimate of the offset of a particular meter, and the uncertainties of the system are built into the filter, making it easy to extract them for any intended use. But there are also downsides to using Kalman filters. The filter requires working with matrices of size $n \times n$ where n is the number of states estimated by the filter. This makes it computationally heavy when the area investigated contains many meters. Fortunately, this can be handled by splitting a utility network into smaller portions and handling these individually. Doing so will often also make intuitive sense for utilities, where suburban streets create natural clusters for the analysis.

3.2. Laplace Domain Tools for Co-Calibration of Sensors in a Network

Conventional calibration methods undertaken in the laboratory require stable conditions and are consequently time consuming and costly to apply. This requirement is hard to achieve in the case of in situ calibration as the realization of steady-state conditions, for example, in the case of a city-wide sensor network is nearly impossible. Furthermore, laboratory calibration of sensors becomes difficult when sensors cannot be removed from the network because it is not physically practical or is too costly to do so. It follows that methods for the co-calibration of sensors under non-static conditions and in situ are needed but such methods require particular mathematical considerations.

A Laplace domain mathematical tool was developed within the 'FunSNM' project for co-calibrating sensors in a sensor network that compensates for the effects of intrinsic differences and time lags between the sensors. Furthermore, the tool makes it possible to obtain the calibration coefficients between sensors in situ. In a case with at least one traceably calibrated sensor, the idea is to obtain the transfer functions of individual sensors from which the calibration coefficients can be calculated. This approach requires the calculation of the overall transfer function between two arbitrary sensors in a period of time, including the so-called transfer function of the medium, and then obtaining the transfer function of the sensor pairs by compensating for the medium.

The overall transfer function H_{ij} between two sensors is written as:

$$H_{ij} = H_{ij}^{m} \cdot H_j / H_i \tag{5}$$

where H_i and H_j denote the transfer functions of the sensors i and j, respectively, and H_{ij}^{m} is the transfer function of the medium between sensors i and j. The numbers of zeros and poles in the transfer functions need to be identified based on the actual physical phenomena under study. For example, in most cases with thermal systems, a first- or second-order transfer function serves ideally for H_{ij}^{m}, while the transfer functions of the sensors depend on factors that define how the sensors transform the actual measurand into the sensor readout, including sensor dynamics, physical characteristics, and electrical characteristics, etc. It is advisable to apply appropriate preprocessing methods to enhance the quality of the signal and employ parameter estimation algorithms to fit the model:

$$H_{ij} = \frac{q_1^{i,j}\left(s - z_1^{i,j}\right)\left(s - z_2^{i,j}\right)}{\left(s - p_1^{i,j}\right)\left(s - p_2^{i,j}\right)} \tag{6}$$

to the sensor readout data. The zeros ($z_{1/2}^{i,j}$), poles ($p_{1/2}^{i,j}$), and constant terms ($q_1^{i,j}$) for each pair of sensors can be written conveniently as the elements of $n \times n$ upper triangular matrices Z_1, Z_2, P_1, P_2 and Q_1, with n denoting the number of sensors, where:

$$Z_1 = \begin{bmatrix} 1 & z_1^{1,2} & z_1^{1,3} & \cdots & \cdots & z_1^{1,n} \\ 0 & 1 & z_1^{2,3} & \cdots & \cdots & z_1^{2,n} \\ \vdots & \vdots & \ddots & \ddots & \ddots & \vdots \\ 0 & 0 & 0 & \cdots & 0 & 1 \end{bmatrix}, \tag{7}$$

and similarly for the other terms.

Since each of the zeros and poles depends solely on either the respective sensor or its position, it follows that:

$$Z_1 = \hat{Z}_1 \cdot \Psi + E_{Z1}, \;\; Z_2 = \Psi \cdot \hat{Z}_2 + E_{Z2}, \;\; P_1 = \hat{P}_1 \cdot \Psi + E_{P1}, \;\; P_2 = \Psi \cdot \hat{P}_2 + E_{P2}, \tag{8}$$

where $\hat{Z}_1$, $\hat{Z}_2$, $\hat{P}_1$ and $\hat{P}_2$ contain the first and second zeros and poles, respectively, stored as diagonal matrices of size n, Ψ is the unit upper triangular matrix (a matrix with zeros below its main diagonal and ones on and above the diagonal), and E_{Z1}, E_{Z2}, E_{P1} and E_{P2} are error matrices that take into account numerical deviations while performing parameter estimation for different pairs of sensors. It also follows that:

$$\overline{Z}_1 = \hat{Z}_1 \cdot \mathbf{1} = \overline{Z}_{1,\text{corr}} + \overline{Z}_{1,\text{uncorr}}, \tag{9}$$

and similarly for the other terms, where **1** is a column vector of ones, in which terms describing correlated effects are distinguished from those representing uncorrelated effects to represent a separation of parameters in the transfer function of the medium from those in the transfer functions for the sensors. Specifically, the term $\overline{Z}_{1,\text{corr}}$ (and, similarly, $\overline{Z}_{2,\text{corr}}$, $\overline{P}_{1,\text{corr}}$ and $\overline{P}_{2,\text{corr}}$) is associated with the medium and is calculated using nonlinear regression models or fitting functions using data-driven approaches. Alternatively, physics-based partial differential equations can be transformed to the Laplace domain to identify the poles and zeros of the transfer function for the medium. For example, for a simplified one-dimensional heat transfer problem in a duct (see Figure 2), the energy balance can be modelled as:

$$\mathcal{L}\left\{\frac{\mathrm{d}}{\mathrm{d}t}\left(\rho V c_p T(t)\right)\right\} = \mathcal{L}\left\{\dot{Q}_{\text{in}} - \dot{Q}_{\text{out}} - q_{\text{loss}}\right\}, \tag{10}$$

where $\mathcal{L}$ denotes the Laplace transformation, ρ is the density of air, V is the confined volume, c_p is the specific heat capacity of air at constant pressure, $T(t)$ is the temperature at time t, and $\dot{Q}_{\text{in}}$, $\dot{Q}_{\text{out}}$ and q_{loss} are the rate of energy in, rate of energy out and the energy loss to the surroundings between the inlet and outlet, respectively. Then, H_{ij}^m can be modelled as follows:

$$H_{ij}^m(s) = \frac{T_{\text{out}}}{T_{\text{in}}} = \frac{\frac{\dot{m}}{\rho V} + x}{s + \frac{\dot{m}}{\rho V} + x}, \tag{11}$$

where $\dot{m}$ is the mass flow rate and x is the heat loss ratio, both identified through parameter identifications, and T_{in} and T_{out} are the temperatures at the inlet and outlet, respectively, of the duct.

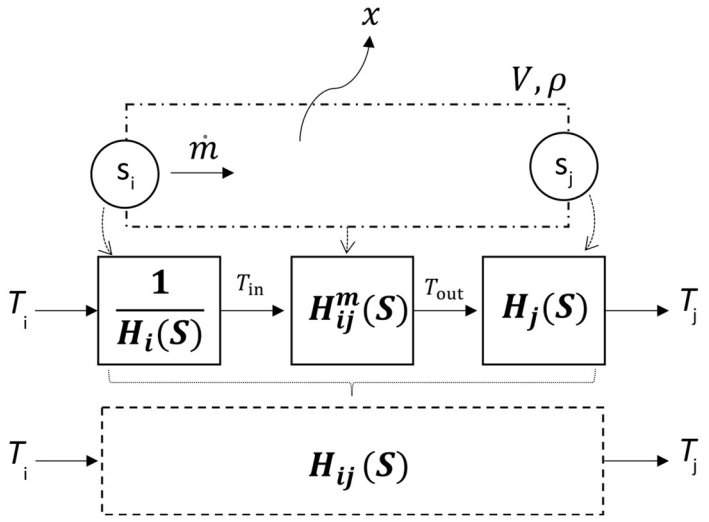

Figure 2. A simplified one-dimensional heat transfer problem in a duct and its representative block diagrams in the Laplace domain. T_i and T_j are the readouts of the temperature sensors s_i and s_j with the transfer functions $H_i(S)$ and $H_j(S)$ passing through a control volume represented by $H_{ij}^m(S)$, where ρ is the density of air, V is the confined volume, $\dot{m}$ is the mass flow rate, x is the heat loss ratio,

and T_{in} and T_{out} are the temperatures at the inlet and outlet, respectively, of the duct. $H_{ij}(S)$ is the transfer function representing the entire system.

As a next step, H_j/H_i is calculated by dividing the overall transfer function H_{ij} by that of the data-driven or physics-based transfer function H_{ij}^m for the medium as given in expression (5). The step response function is calculated by applying the inverse Laplace domain transform and evaluating its horizontal asymptote y_i^∞. A first estimation of the calibration matrix $\overline{C}$ is then obtained by dividing those terms in pairs:

$$\overline{C} = \begin{bmatrix} 1 & y_2^\infty/y_1^\infty & y_3^\infty/y_1^\infty & \cdots & \cdots & y_n^\infty/y_1^\infty \\ 0 & 1 & y_3^\infty/y_2^\infty & \cdots & \cdots & y_n^\infty/y_2^\infty \\ \vdots & \vdots & \ddots & \ddots & \ddots & \vdots \\ 0 & 0 & 0 & \cdots & 0 & 1 \end{bmatrix}, \tag{12}$$

and it can be shown that:

$$\overline{C}_{ij} = \frac{y_j^\infty}{y_i^\infty} = \frac{\frac{q^j z_1^j z_2^j}{p_1^j p_2^j}}{\frac{q^i z_1^i z_2^i}{p_1^i p_2^i}}. \tag{13}$$

The relative standard uncertainty for each calibration coefficient term $\overline{C}_{ij}$ in this estimation is:

$$u_{\overline{C}_{ij},r} = \sqrt{\sum u_{q,r}^2 + \sum u_{z,r}^2 + \sum u_{p,r}^2}, \tag{14}$$

where the summations are taken over all parameters for both sensors.

Finally, using the results (12) and (13) from the first estimation, the expression:

$$\overline{C} = \begin{bmatrix} 1 & c_2/c_1 & c_3/c_1 & \cdots & \cdots & c_n/c_1 \\ 0 & 1 & c_3/c_2 & \cdots & \cdots & c_n/c_2 \\ \vdots & \vdots & \ddots & \ddots & \ddots & \vdots \\ 0 & 0 & 0 & \cdots & 0 & 1 \end{bmatrix} \tag{15}$$

defines an overdetermined system of equations that is solved for estimates of the calibration coefficients $c_i, i = 1, \ldots, n$, for the individual sensors and reported with an associated covariance matrix. The covariance matrix gives information about the uncertainty of the estimates, which captures contributions from all parameters (zeros, poles, and constants) in the transfer functions for the sensor pairs and for the medium between the sensors.

3.3. Accounting for Correlation in the Measurements Made by the Sensors in a Network

When evaluating the uncertainty of a measurand it is important to properly address the correlations that may exist between the various input quantities on which the measurand depends. In the case of sensor networks, such correlations often arise as such networks typically contain multiple sensors of the same make, measuring the same quantity at different locations, experiencing similar ambient conditions, and the sensors are possibly calibrated or tested against the same reference instrument. Furthermore, the measurement errors affecting the readings of a single sensor at different temporal points are likely to be correlated. If multiple readings from sensors are used as inputs to a measurement model, for example, for the calculation of an aggregate quantity such as an overall average or for estimating an interpolated value, then correlations between these inputs should be properly treated.

Here, the focus is on the statistical correlation of measurement errors made by different sensors, or of measurement errors made by the same sensor at different temporal points. To make this more precise, let Y_{ij} denote the measurand evaluated at spatial location

$\boldsymbol{s}_i = (x_i, y_i, z_i)$ with $1 \leq i \leq m$ and temporal point t_j with $1 \leq j \leq n$, i.e., $Y_{ij} = Y(\boldsymbol{s}_i, t_j)$. Furthermore, let the corresponding sensor reading be X_{ij} whereby the sensor that is permanently installed at spatial location $\boldsymbol{s}_i$ is denoted by sensor i, and let the measurement error be E_{ij}, i.e., $X_{ij} = Y_{ij} + E_{ij}$. The correlation that is of interest is the correlation in the E_{ij}. Generally, this is different from the correlation in the data X_{ij}. In the special case that the measurand Y_{ij} is independent of space and time, i.e., constant, then these correlations are equal. The time series $(x_{i_1,j})_{1\leq j\leq n}$ and $(x_{i_2,j})_{1\leq j\leq n}$, as concrete sets of n observations (measured values) of the random variables $X_{i_1,j}$ and $X_{i_2,j}$ corresponding to sensors i_1 and i_2, can be strongly correlated if the true values $(y_{i_1,j})_{1\leq j\leq n}$ and $(y_{i_2,j})_{1\leq j\leq n}$ of the measurands are themselves highly correlated and if their variations are larger than the typical size of the measurement errors. For example, if two sensors monitor ambient temperature at nearby spatial locations where the temperature is almost identical, and the temperature is strongly varying, then the readings of these temperature sensors will be highly correlated, independently of the presence or absence of correlation in their measurement errors. However, to determine the uncertainty of the mean temperature, correlation information with respect to the measurement errors is required.

In the analysis of sensor network data, it is often assumed that the measurement errors of the sensors in a sensor network are independent and identically distributed (i.i.d.) and described by a Gaussian distribution. This assumption is not always realistic, and it can lead to inaccurate results. The measurement uncertainties calculated for aggregated and interpolated values of the measurand at different spatial locations and temporal points can be appreciably different when using a model that accounts for correlations in measurement errors compared to the standard (Gaussian) i.i.d. sensor noise model.

The measurement errors for the m sensors, indexed by i with $1 \leq i \leq m$ at the n temporal points indexed by j with $1 \leq j \leq n$, can be modelled as a multivariate Gaussian distribution with mean zero and an $mn \times mn$ dimensional covariance matrix V. To make this covariance matrix manageable and easy to evaluate for arbitrary spatial locations $\boldsymbol{s}_i$ and temporal points t_j, the kernel function arising in Gaussian process modelling [51] can be used. Such a function returns the covariance of, in this case, the measurement errors for any combination of two inputs $(\boldsymbol{s}_{i_1}, t_{j_1})$ and $(\boldsymbol{s}_{i_2}, t_{j_2})$ defining two points in spacetime. To select an appropriate shape of the kernel function and to estimate the values of its free parameters $\boldsymbol{\alpha}$, it is required that a sample of the measurement errors is available. This can be the case when the sensor readings are compared with low-uncertainty reference instrumentation, the latter providing a good proxy for the true values of the measurands. To be able to determine an appropriate covariance structure for both the spatial and temporal directions, the dataset should include variations in all relevant variables, i.e., in both space and time. In concrete cases when there is not enough experimental data, for example, when all measurements have been performed at a single location, some expert-based assumptions may be needed to construct a reasonable functional structure and parameter values for the kernel function $k_E\big((\boldsymbol{s}_{i_1}, t_{j_1}), (\boldsymbol{s}_{i_2}, t_{j_2}); \boldsymbol{\alpha}\big)$ giving the covariance of the measurement errors E_{i_1,j_1} and E_{i_2,j_2}. Figure 3 shows an example, based on the QUANT dataset [52] using data from low-cost air quality measurements combined with reference data provided on the same website, of a kernel function with respect to time, accounting for periodicity in the observations (which can be caused by daily patterns), as well as a kernel function with respect to space, where the correlation decays the further two sensors are removed from each other.

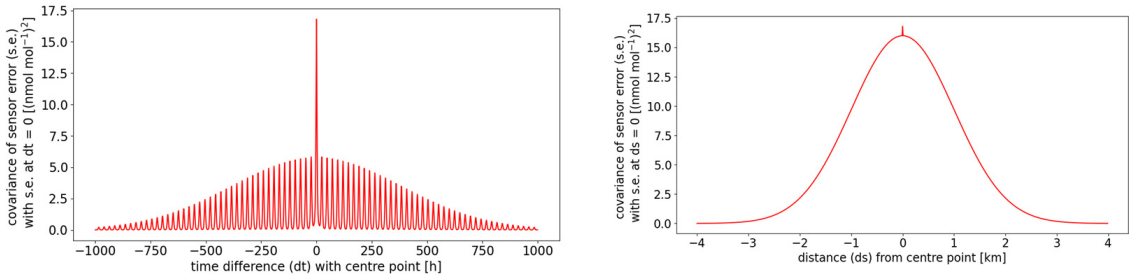

(**a**) (**b**)

Figure 3. Crosscuts of an example kernel function that describes the covariance between sensor errors for different points in time and space: (**a**) the time component follows a decaying periodic structure, while (**b**) the space component follows a decaying structure.

When fitting the kernel parameters $\boldsymbol{\alpha}$, the value of the noise parameter for the observed values e_{ij} of the measurement errors can be set to the uncertainty of the reference measurements. Once the structure and parameters of the kernel function are fixed, this function can be used to calculate the covariance matrix for any finite set of measurements taken by the sensors at different spatial locations and temporal points. This covariance matrix can then be used as part of the input to a measurement model depending on a set of sensor readings, for example, for the calculation of an average value. In [53], this was performed for calculating the average amount fraction of nitrogen dioxide (NO_2) in air as measured by NO_2 sensors in a sensor network for air quality monitoring. In this research, ignoring the between-sensor and within-sensor correlations led to an uncertainty of the average NO_2 amount fraction that was more than ten times lower than the uncertainty of the average NO_2 amount fraction when taking the correlation structure properly into account.

Another possibility for using the kernel function k_E arises when one decides to model the measurand $Y(\boldsymbol{s}, t)$ and the sensor readings X_{ij} themselves by a Gaussian process. In this case the kernel function k_E can be used as part of a larger kernel function k_X that models the covariance structure of the observed data, i.e., the terms contained in k_E are part of the terms contained in k_X. This would then replace the purely Gaussian i.i.d. noise model that is typically assumed in Gaussian process modelling. To illustrate this approach, a comparison was made between three inference methods on a synthetic dataset, generated by a Gaussian process with a known kernel function. In this dataset, 100 sensors are located in an area of 10 km by 10 km and the measurand is defined as the NO_2 amount fraction at the centre of this area (see Figure 4). To evaluate the uncertainty of the measurand, three different Gaussian processes were assumed. The kernel function of the first Gaussian process matches the kernel function of the Gaussian process used to generate the data, the second Gaussian process assumes that the sensor errors are i.i.d. Gaussian distributed, while the third Gaussian process does not assume knowledge about the sensor errors, i.e., the stochastic behaviour of the true values of the measurand and of the sensor errors are confounded. The hyperparameters of all kernel functions are determined using the observed data. This process was repeated 10,000 times to obtain robust results. The results indicate that the choice of model function does not have a large effect on the estimate of the NO_2 amount fraction. However, the uncertainty of the NO_2 amount fraction does depend on the choice of Gaussian process. When using the correct kernel, the true NO_2 amount fraction was included in the 95% coverage interval for approximately 95% of the results. However, assuming i.i.d. Gaussian sensor errors led to an overestimation of the uncertainty, resulting in a coverage rate of 98%. When making no assumptions on the sensor errors led to an underestimation of the uncertainty, resulting in a coverage rate of 90%. In conclusion, in order to obtain an accurate evaluation of the uncertainty, it is crucial to take sensor error correlations correctly into account.

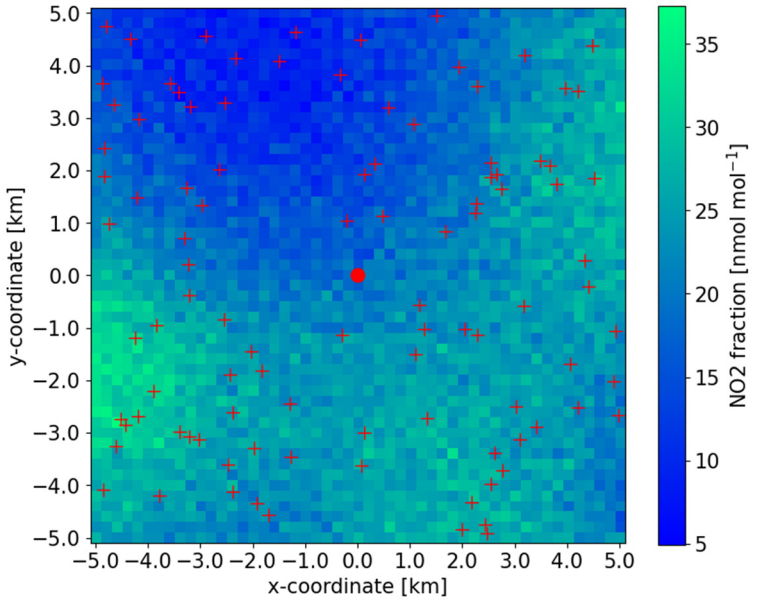

Figure 4. Example heatmap of the true NO_2 amount fractions in the synthetic dataset, including the sensor locations and point of interest.

3.4. Drift Estimation for the Sensors in a Network

Sensor drift is a ubiquitous challenge to the proper treatment of sensor network data. Sensor drift often arises in networks comprising low-cost sensors [54–56], but it can also be present in networks comprising state-of-the-art sensors deployed in harsh environments. An example of the latter are thermocouples used to measure the temperature within furnaces in the manufacture of high-value engineering components.

A thermocouple comprises two dissimilar metal wires joined together at one end to form a measurement junction with the reference junction at the other end at 0 °C. A voltage, which is a function of the temperature gradient between the two ends, is developed across the wires and measured at the open end. Each wire develops an electromotive force (emf) [57] in a temperature gradient, which is the thermoelectric effect. For any small length of wire this emf is the product of the Seebeck coefficient, which is characteristic of a given metal, and the temperature difference from one end of that length of wire to the other [58].

Thermocouples made of platinum (Pt) and its alloys with rhodium (Pt-Rh) are widely used in high value manufacturing applications as they offer relatively high thermoelectric stability in comparison with other thermocouples, particularly at temperatures above approximately 1000 °C. For example, noble metal thermocouples typically drift by tenths or hundredths of a °C per month on continuous exposure above this temperature, whereas less expensive thermocouples can typically drift by more than ten or a hundred times as much in the same period. The principal cause of drift in noble metal thermocouples is vaporization of Pt and Rh oxides from the wires, which causes a local change in composition, and hence, in the Seebeck coefficient [59,60]. The magnitude of this effect depends on the Pt-Rh composition of the wire. A thermocouple assembly can comprise several wires. For example, a 5-wire thermocouple with the widely available compositions Pt0%Rh (or Pt), Pt6%Rh, Pt10%Rh, Pt13%Rh and Pt30%Rh offers 10 possible pairs of wires and so 10 thermocouples (see Figure 5). As there is some commonality across the multi-wire thermocouples (e.g., a Pt6%Rh versus Pt30%Rh thermocouple and a Pt6%Rh versus Pt13%Rh thermocouple shares a Pt6%Rh wire), the question is whether the resulting correlations between the measurements made by different thermocouples in the ensemble can be employed to provide useful information about drift and an improved (lower uncertainty) measurement of temperature.

Figure 5. Schematic of a five-wire thermocouple assembly. The voltage can be measured across any two wires to make an individual thermocouple. All thermocouples are measuring the same temperature because they share a common measurement junction. (The pure platinum wire Pt0%Rh is labelled as Pt).

A model for the temperature drift at each time $t_i, i = 1, \ldots, n_t$, for the k^{th} of m thermocouples in a multi-wire thermocouple is:

$$T_{i,k} + e_{i,k} = T_i + \delta T_{i,k}, \quad k = 1, \ldots, m, \tag{16}$$

where $T_{i,k}$ is the measured value of temperature drift, $e_{i,k}$ is a random draw from the Gaussian distribution $\mathrm{N}(0, \sigma_{\mathrm{T}}^2)$ with mean zero and variance σ_{T}^2, T_i is the unknown temperature common to all thermocouples, and $\delta T_{i,k}$ is the unknown temperature drift for the kth thermocouple. In this model, each of the values $T_{i,k}$, T_i and $\delta T_{i,k}$ is taken to be relative to the temperature at an initial time t_0 at which all the thermocouples record the same temperature and at which there is no temperature drift.

The problem is similar to a Key Comparison (KC) of the measurements made by m laboratories of a property (temperature) of a single artefact. One way to obtain a unique solution is to include one additional piece of information, for example, that on average the temperature drift of a thermocouple is zero:

$$\sum_{k=1}^{m} \delta T_{i,k} = 0. \tag{17}$$

It then follows that an estimate of the temperature T_i—akin to the reference or consensus value in a key comparison—is evaluated as the average of the measured temperature drifts and estimates of the temperature drifts—akin to the laboratory degrees of equivalence in a key comparison—are evaluated as the differences between the measured temperature drifts and their average. In this approach, which is purely 'data-driven', the additional information represented by the condition (17) is empirical and might not represent the true behaviour of the sensors. Consideration is now given to how the condition can be replaced by knowledge that is 'physics-driven' and descriptive of the real behaviour of the thermocouples in the multi-wire thermocouple.

The physics-based model described in [61] provides information about the relative temperature drift of two thermocouples in the form:

$$\delta T_{i,k} = \beta_k \delta T_{i,1}, \quad k = 1, \ldots, m, \tag{18}$$

with $\beta_1 \equiv 1$. Here, β_k is known from knowledge of the compositions of the wires making up the thermocouples and is independent of temperature.

To begin with, consider the case that the $\beta_k, k = 2, \ldots, m$, are known. Then, expressions (16) and (18) give:

$$T_{i,k} + e_{i,k} = T_i + \beta_k \delta T_{i,1}, \quad k = 1, \ldots, m, \tag{19}$$

and T_i and $\delta T_{i,1}$ at each time t_i are obtained as the solution to the linear least-squares problem:

$$\min_{T_i, \delta T_{i,1}} \sum_{k=1}^{m} (T_{i,k} - T_i - \beta_k \delta T_{i,1})^2. \tag{20}$$

In this formulation of the drift estimation problem, all the available physics-based knowledge is used.

Alternatively, consider the case that the $\beta_k, k = 2, \ldots, m$, are unknown. Then, expressions (16) and (18) give:

$$T_{i,k} + e_{i,k} = \beta_k (T_{i,1} + e_{i,1}) + (1 - \beta_k) T_i, \quad k = 2, \ \ldots, \ m, \tag{21}$$

which defines a regression problem involving $(m - 1)$ equations and m unknowns. By combining the data for n_t consecutive times, the following non-linear least-squares problem is formulated:

$$\min_{T^*_{i,1}, T_i, \beta_k} \sum_{i=1}^{n_t} \left[\left(T_{i,1} - T^*_{i,1}\right)^2 + \sum_{k=2}^{m} \left(T_{i,k} - \beta_k T^*_{i,1} - (1 - \beta_k) T_i\right)^2 \right] + \lambda \sum_{k=2}^{m} (\beta_k - \beta_{0,k})^2, \tag{22}$$

where $\beta_{0,k}$ are prior values for the β_k provided by the physical model. This formulation makes use of the physics-based knowledge described by expression (18) but allows for the estimation of the parameters $\beta_k, k = 2, \ldots, m$, as well as the temperatures $T_i, i = 1, \ldots, n_t$, common to the thermocouples. The second term in expression (22) is a regularization term that ensures a unique solution, and the parameter λ is used to control the weighting of the prior knowledge with respect to the measurements $T_{i,k}$ of temperature drift. In this formulation of the drift estimation problem, use is made of partial physics-based knowledge together with data from consecutive measurement times to replace some of the physics-based knowledge used before.

In all these cases, the drift estimation problem is formulated as an inverse problem and in the form of either a linear or non-linear least-squares regression problem. Methods based on maximum likelihood estimation or Bayesian statistics [62] allow the proper treatment of uncertainties when solving such problems. For example, in a Bayesian analysis, prior probability distributions for the model parameters are updated using measured data, with information about the measured data captured in a likelihood function that depends on the measurement uncertainties, to obtain a posterior distribution for the parameters.

To illustrate the approaches, measured values of temperature drift were collected from eight thermocouples in a 5-wire thermocouple as illustrated in Figure 5 [63]. The data were obtained while the thermocouple was immersed in a calibration artefact (a cobalt-carbon fixed-point cell with a melting temperature of 1324.29 °C) and recorded over a time period of about 500 h. The study focused on the time period between about 200 h and 500 h with data at the start of the time period omitted, as in that early period, there can be mechanisms (other than evaporation) that cause the observed calibration drift. The estimates of temperature at each time point obtained from the three approaches described, and the standard uncertainties associated with those estimates, are shown in Figure 6. The estimates obtained from the approach 'Unknown β' (based on solving expression (22)) are better than those from approach 'Known β' (based on solving expression (20) for each time t_i) that are in turn better than those from approach 'KC', and so suggest there is benefit in including physics knowledge in the estimation problem. The results indicate that including more physics knowledge does not necessarily translate into smaller uncertainties associated with the estimates of temperature the uncertainties are largest for the approach 'Unknown β', although we might hope for more 'realistic' uncertainties in that case. A more comprehensive comparison of the methods described above, including other methods,

using data collected from different multi-wire thermocouples subject measuring in different temperature environments is currently underway and will be reported elsewhere.

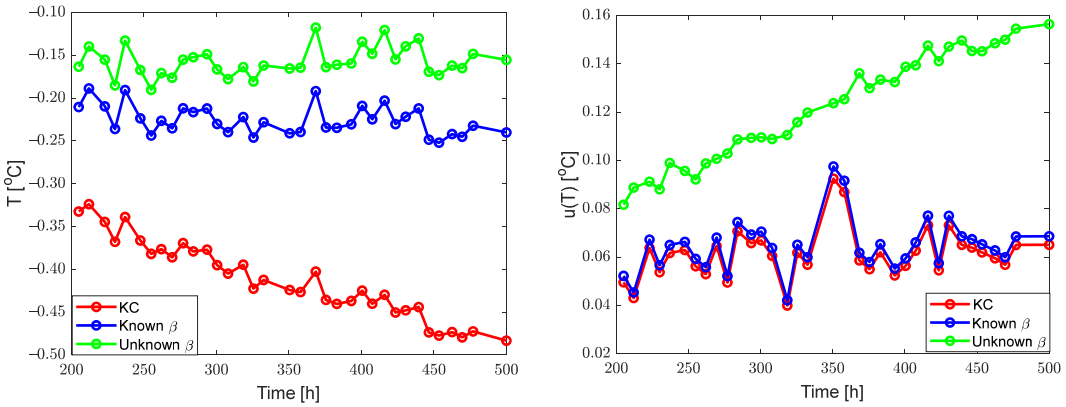

Figure 6. For the three approaches, (**a**) Estimates of temperature shown as differences from the cobalt-carbon fixed-point of 1324.29 °C, and (**b**) associated standard uncertainties.

4. Summary and Conclusions

Sensor networks are increasingly being used in a broad range of applications, such as smart cities, environmental monitoring, and advanced manufacturing. Sensor networks constitute a metrology paradigm that involves an ensemble of sensors measuring possibly different quantities at a discrete sample of spatial locations and temporal points under conditions that differ from those in the laboratory. Results from sensor networks, as for any measuring system, need to be accompanied by reliable statements of measurement uncertainty. This is especially crucial when sensor networks are to be considered as true metrology systems and their measurement results are to be used for decision-making, such as in a regulatory context.

This paper has given a preview of some of the work undertaken within the European-funded 'FunSNM' project to address the challenges of measurement uncertainty evaluation in some real-world sensor network applications. Those challenges—related to the nature of the measured quantities, of the measurement model, and of the measured data—make conventional methods for modelling and established methods and guidelines for measurement uncertainty evaluation (e.g., GUM) difficult to apply.

The applications illustrate the use of different modelling and statistical tools to address the challenges of measurement uncertainty evaluation for sensor networks. These tools include (i) Kalman filters for estimating the state of utility networks in urban environments, such as a district heating network with a tree-based topology, (ii) Laplace domain tools for the in situ co-calibration of sensors in a network, (iii) Gaussian process models for describing the correlations between the measurements made by sensors in a network, such as for air quality monitoring, and (iv) inverse (least-squares) problems for undertaking the aggregation of data from sensors in a network, for example, to estimate the calibration drift of thermocouples for temperature measurement in high-value manufacturing.

The Kalman filter in its various guises is a useful tool to estimate the state of a system using data collected by a sensor network, but it is not easily represented in the form of the measurement models treated by the GUM. However, the filter provides a treatment of sensor network data that is naturally 'uncertainty-aware', as it allows the update and tracking of the estimates of the filter state variables and their associated measurement uncertainties at each filter step. Model transforms, such as the Laplace transform described in this work, can be used to capture sensor dynamics and sensor behaviour. Although

the model transforms are not easily represented in the form of a GUM measurement model, similarly to the Kalman filter, this article indicated how measurement uncertainty can be evaluated in the context of such model transforms. Conventional approaches to representing uncertainty information about measured data, such as the use of correlation matrices, do not scale well to the large volumes of data collected by sensor networks. It is demonstrated how Gaussian process models provide a useful tool to describe, and distinguish between, the spatial and temporal correlations in the errors in sensor data and in the quantities measured by the sensors. Finally, the decisions made using sensor network data often depend on solving an inverse problem by least-squares. The current GUM suite of documents does not include a dedicated treatment of such problems, but statistical tools based on maximum likelihood or Bayesian estimation as being developed within the FunSNM project can be used to provide an evaluation of measurement uncertainty for the solutions to such problems. In summary, the methods developed by the FunSNM project enable uncertainty evaluation in various complex situations as encountered in sensor networks, where traditional models fall short due to the size of the problem, the complexity of the physics and the involved dynamics.

Author Contributions: Conceptualization, P.H. and S.T.; investigation (incl. methodology, software, validation, formal analysis and resources) for Section 3.1, P.F.Ø.; investigation (incl. methodology, software, validation, formal analysis and resources) for Section 3.2, S.T. and H.S.; investigation (incl. methodology, software, validation, formal analysis and resources) for Section 3.3, G.K. and M.v.D.; investigation (incl. methodology, software, validation, formal analysis and resources) for Section 3.4, P.H., Y.L., J.P. and D.T.; writing—original draft preparation, P.H., P.F.Ø., S.T., G.K., A.P.V. and M.I.-G.; writing—review and editing, P.H., P.F.Ø., S.T., H.S., G.K., M.v.D., Y.L., J.P., D.T., A.P.V. and M.I.-G. All authors have read and agreed to the published version of the manuscript.

Funding: The project (22DIT02 FunSNM) has received funding from the European Partnership on Metrology, co-financed from the European Union's Horizon Europe Research and Innovation Programme and by the Participating States.

Data Availability Statement: The datasets used for the examples described in Sections 3.1 and 3.2 are not readily available because the data are part of an ongoing study. Requests to access those datasets should be directed to the authors. The publicly available dataset [52] was used for the example described in Section 3.3. The dataset used for the example described in Section 3.4 is available in the public repository [63].

Conflicts of Interest: The authors declare no conflicts of interest. The funders had no role in the design of the study; in the collection, analyses, or interpretation of data; in the writing of the manuscript; or in the decision to publish the results.

References

1. BIPM; IEC; IFCC; ILAC; ISO; IUPAC; IUPAP; OIML. *International Vocabulary of Metrology—Basic and General Concepts and Associated Terms*; Joint Committee for Guides in Metrology, JCGM: Paris, France, 2012; p. 200.
2. de Bièvre, P.; Taylor, P.D.P. Traceability to the SI of amount-of-substance measurements: From ignoring to realizing, a chemist's view. *Metrologia* **1997**, *34*, 67–75. [CrossRef]
3. Brewer, P.J.; Brown, R.J.C.; Tarasova, O.A.; Hall, B.; Rhoderick, G.C.; Wielgosz, R.I. SI traceability and scales for underpinning atmospheric monitoring of greenhouse gases. *Metrologia* **2018**, *55*, S174–S181. [CrossRef]
4. Tabandeh, S.; Vedurmudi, A.P.; Söderblom, H.; Purjamal, S.; Harris, P.; Gruber, M.; Vaa, M.; Johansen, M.; Koval, M.; Østergaard, P.F.; et al. Sensor network metrology: Current state and future directions. In Proceedings of the XXIV IMEKO World Congress, Hamburg, Germany, 26–29 August 2024.
5. Rietveld, G.; Braun, J.-P.; Martin, R.; Wright, P.; Heins, W.; Ell, N.; Clarkson, P.; Zisky, N. Measurement infrastructure to support the reliable operation of smart electrical grids. *IEEE Trans. Instrum. Meas.* **2015**, *64*, 1355–1363. [CrossRef]
6. Powell, J.; McCafferty-Leroux, A.; Hilal, W.; Gadsden, S.A. Smart Grids: A Comprehensive Survey of Challenges, Industry Applications, and Future Trends. 2024. Available online: http://arxiv.org/abs/2401.13105 (accessed on 1 June 2024).

7. RELaTED Project—New Heating and Cooling Solutions. Available online: https://www.relatedproject.eu/ (accessed on 23 July 2024).
8. Johra, H.; Leiria, D.; Heiselberg, P.; Marszal-Pomianowska, A.; Tvedebrink, T. Treatment and analysis of smart energy meter data from a cluster of buildings connected to district heating: A Danish case. In *12th Nordic Symposium on Building Physics, NSB 2020, Tallinn, Estonia, 6–9 September 2020*; EDP Sciences: Paris, France, 2020.
9. Ali, A. A framework for air pollution monitoring in smart cities by using IoT and smart sensors. *Informatica* **2022**, *46*, 129–138. [CrossRef]
10. Ramos, F.; Trilles, S.; Muñoz, A.; Huerta, J. Promoting Pollution-Free Routes in Smart Cities Using Air Quality Sensor Networks. *Sensors* **2018**, *18*, 2507. [CrossRef]
11. Wang, D.; Agrawal, D.P.; Toruksa, W.; Chaiwatpongsakorn, C.; Lu, M.; Keener, T.C. Monitoring ambient air quality with carbon monoxide sensor-based wireless network. *Commun. ACM* **2010**, *53*, 138–141. [CrossRef]
12. Boubrima, A.; Bechkit, W.; Rivano, H.; Ruas, A. Wireless sensor networks deployment for air pollution monitoring. In Proceedings of the TAP 2016-21st International Transport and Air Pollution Conference, Lyon, France, 24–26 May 2016.
13. Xu, G.; Shen, W.; Wang, X. Applications of wireless sensor networks in marine environment monitoring: A survey. *Sensors* **2014**, *14*, 16932–16954. [CrossRef]
14. Woo-García, R.M.; Pérez-Vista, J.M.; Sánchez-Vidal, A.; Herrera-May, A.L.; Osorio-de-la-Rosa, E.; Caballero-Briones, F.; López-Huerta, F. Implementation of a wireless sensor network for environmental measurements. *Technologies* **2024**, *12*, 41. [CrossRef]
15. Prabhu, B.; Praddep, M.; Gajendran, E. Monitoring climatic conditions using wireless sensor networks. *Multidiscip. J. Sci. Res. Educ.* **2017**, *3*, 179–184.
16. Walid, F.; Ezzedine, T. Design of a climate monitoring system based on sensor network. In Proceedings of the 13th International Wireless Communications and Mobile Computing Conference (IEEE-IWCMC), Valencia, Spain, 26–30 June 2017; pp. 1791–1796. [CrossRef]
17. Vyas, K.; Shukla, S.; Dsouza, H.; Dsouza, D.; Narnaware, V. A survey on environment monitoring using sensor networks. *Asian J. Converg. Technol.* **2020**, *6*, 95–99. [CrossRef]
18. Eichstädt, S. Metrology for the Factory of the Future. Available online: https://researchoutreach.org/wp-content/uploads/2021/10/Metrology-for-the-Factory-of-the-Future.pdf (accessed on 23 July 2024).
19. Eichstädt, S.; Ludwig, B. Metrology for heterogeneous sensor networks and Industry 4.0. *Automatisierungstechnik* **2020**, *68*, 459–464. [CrossRef]
20. Majid, M.; Habib, S.; Javed, A.R.; Rizwan, M.; Srivastava, G.; Gadekallu, T.R.; and Lin, J.C.-W. Applications of Wireless Sensor Networks and Internet of Things Frameworks in the Industry Revolution 4.0: A Systematic Literature Review. *Sensors* **2022**, *22*, 2087. [CrossRef] [PubMed]
21. Ozdemir, S.; and Xiao, Y. Secure data aggregation in wireless sensor networks: A comprehensive overview. *Comput. Netw.* **2009**, *53*, 2022–2037. [CrossRef]
22. Chen, Y.; Shu, J.; Zhang, S.; Liu, L.; Sun, L. Data fusion in wireless sensor networks. In Proceedings of the Second International Symposium on Electronic Commerce (IEEE-ISECS), Nanchang, China, 22–24 May 2009; pp. 504–509. [CrossRef]
23. Eichstädt, S.; Vedurmudi, A.P.; Gruber, M.; Hutzschenreuter, D. Fundamental aspects in sensor network metrology. *Acta IMEKO* **2023**, *12*, 1–6. [CrossRef]
24. Lin, C.; Gillespie, J.; Schuder, M.D.; Duberstein, W.; Beverland, I.J.; Heal, M.R. Evaluation and calibration of Aeroqual series 500 portable gas sensors for accurate measurement of ambient ozone and nitrogen dioxide. *Atmos. Environ.* **2015**, *100*, 111–116. [CrossRef]
25. Topalović, D.B.; Davidović, M.D.; Jovanović, M.; Bartonova, A.; Ristovski, Z.; Jovašević-Stojanović, M. In search of an optimal in-field calibration method of low-cost gas sensors for ambient air pollutants: Comparison of linear, multilinear and artificial neural network approaches. *Atmos. Environ.* **2019**, *213*, 640–658. [CrossRef]
26. Tancev, G.; Ackermann, A.; Schaller, G.; Pascale, C. Efficient and automated generation of orthogonal atmospheres for the characterization of low-cost gas sensor systems in air quality monitoring. *IEEE Trans. Instrum. Meas.* **2022**, *71*, 1006410. [CrossRef]
27. European Partnership on Metrology. Available online: https://www.euramet.org/research-innovation/metrology-partnership (accessed on 23 July 2024).
28. Fundamental Principles of Sensor Network Metrology. Available online: https://www.euramet.org/research-innovation/search-research-projects/details/project/fundamental-principles-of-sensor-network-metrology (accessed on 23 July 2024).
29. Eichstädt, S.; Makarava, N.; Elster, C. On the evaluation of uncertainties for state estimation with the Kalman filter. *Meas. Sci. Technol.* **2016**, *27*, 125009. [CrossRef]
30. Kok, G.; Harris, P. Uncertainty evaluation for metrologically redundant industrial sensor networks. In Proceedings of the IEEE International Workshop on Metrology for Industry 4.0 & IoT, Roma, Italy, 3–5 June 2020. [CrossRef]

31. Yong, B.X.; Brintrup, A. Multi agent system for machine learning under uncertainty in cyber physical manufacturing system; Service Oriented, Holonic and Multi-agent Manufacturing Systems for Industry of the Future. In Proceedings of the SOHOMA 2019, Valencia, Spain, 3–4 October 2019; Springer International Publishing: Berlin/Heidelberg, Germany, 2020; p. 9.
32. Ni, F.; Nguyen, P.H.; Cobben, J.F.G.; van den Brom, H.E.; Zhao, D. Uncertainty analysis of aggregated smart meter data for state estimation. In Proceedings of the IEEE International Workshop on Applied Measurements for Power Systems (AMPS), Aachen, Germany, 28–30 September 2016; pp. 1–6. [CrossRef]
33. Dorst, T.; Schneider, T.; Schutze, A. D1. 1 GUM2ALA—Uncertainty propagation algorithm for the adaptive linear approximation according to the GUM. In *SMSI 2021—System of Units and Metrological Infrastructure*; AMA: Chicago, IL, USA, 2021. [CrossRef]
34. Eichstädt, S.; Werhahn, O. Metrology for sensor networks: Metrological traceability and measurement uncertainties for air quality monitoring. *Tm Tech. Mess.* **2024**, *91*, 419–429. [CrossRef]
35. BIPM; IEC; IFCC; ILAC; ISO; IUPAC; IUPAP; OIML. *Evaluation of Measurement Data—Guide to the Expression of Uncertainty in Measurement*; Joint Committee for Guides in Metrology, JCGM: Paris, France, 2008; p. 100.
36. Satterthwaite, F.E. An approximate distribution of estimates of variance components. *Biom. Bull.* **1946**, *2*, 110–114. [CrossRef]
37. Welch, B.L. The generalization of 'Student's' problem when several different population variances are involved. *Biometrika* **1947**, *34*, 28–35. [CrossRef] [PubMed]
38. BIPM; IEC; IFCC; ILAC; ISO; IUPAC; IUPAP; OIML. *Evaluation of Measurement Data—Supplement 1 to the "Guide to the Expression of Uncertainty in Measurement"—Propagation of Distributions Using a Monte Carlo Method*; Joint Committee for Guides in Metrology, JCGM: Paris, France, 2008; p. 101.
39. Singh, J.; Kumaraswamidhas, L.A.; Bura, N.; Sharma, N.D. A Monte Carlo simulation investigation on the effect of the probability distribution of input quantities on the effective area of a pressure balance and its uncertainty. *Measurement* **2021**, *172*, 108853. [CrossRef]
40. Rasmussen, K.; Kondrup, J.B.; Allard, A.; Demeyer, S.; Fischer, N.; Barton, E.; Partridge, D.; Wright, L.; Bär, M.; Fiebach, A.; et al. Novel Mathematical and Statistical Approaches to Uncertainty Evaluation: Best Practice Guide to Uncertainty Evaluation for Computationally Expensive Models. 2015. Available online: https://www.ptb.de/emrp/new04-publicationsb345.html (accessed on 1 June 2024).
41. BIPM; IEC; IFCC; ILAC; ISO; IUPAC; IUPAP; OIML. *Evaluation of Measurement Data—Supplement 2 to the "Guide to the Expression of Uncertainty in Measurement"—Extension to Any Number of Output Quantities*; Joint Committee for Guides in Metrology, JCGM: Paris, France, 2011; p. 102.
42. Bartoli, C.; Beug, M.F.; Bruns, T.; Elster, C.; Esward, T.; Klaus, L.; Knott, A.; Kobusch, M.; Saxholm, S.; Schlegel, C. Traceable dynamic measurement of mechanical quantities: Objectives and first results of this European project. *Int. J. Metrol. Qual. Eng.* **2012**, *3*, 127–135. [CrossRef]
43. Elster, C.; Link, A. Uncertainty evaluation for dynamic measurements modelled by a linear time-invariant system. *Metrologia* **2008**, *45*, 464–473. [CrossRef]
44. Eichstädt, S.; Elster, C.; Esward, T.J.; Hessling, J.P. Deconvolution filters for the analysis of dynamic measurement processes: A tutorial. *Metrologia* **2010**, *47*, 522. [CrossRef]
45. Römer, K.; Blum, P.; Meier, L. Time synchronization and calibration in wireless sensor networks. In *Handbook of Sensor Networks: Algorithms and Architectures*; Zomaya, I., Ed.; John Wiley & Sons: Hoboken, NJ, USA, 2005; pp. 199–237. [CrossRef]
46. Jagan, K.; Wright, L.; Harris, P. A Bayesian approach to account for timing effects in industrial sensor networks. In Proceedings of the IEEE International Workshop on Metrology for Industry 4.0 & IoT, Roma, Italy, 3–5 June 2020. [CrossRef]
47. Cofta, P.; Karatzas, K.; Orłowski, C. A conceptual model of measurement uncertainty in IoT sensor networks. *Sensors* **2021**, *21*, 1827. [CrossRef]
48. Kalman, R.E. A New Approach to Linear Filtering and Prediction Problems. *Trans. ASME J. Basic Eng.* **1960**, *82*, 34–45. [CrossRef]
49. Smith, G.L.; Schmidt, S.F.; McGee, L.A. *Application of Statistical Filter Theory to the Optimal Estimation of Position and Velocity on Board a Circumlunar Vehicle*; National Aeronautics and Space Administration: Washington, DC, USA, 1962.
50. Julier, S.J.; Uhlmann, J.K. Unscented Filtering and Nonlinear Estimation. *Proc. IEEE* **2004**, *92*, 401–422. [CrossRef]
51. Rasmussen, C.E.; Williams, C.K.I. *Gaussian Processes for Machine Learning*; The MIT Press: Cambridge, MA, USA, 2006; ISBN 026218253X. Available online: www.GaussianProcess.org/gpml (accessed on 1 June 2024).
52. Lacy, S.; Diez, S.; Edwards, P. Quantification of Utility of Atmospheric Network Technologies: (QUANT): Low-Cost Air Quality Measurements from 52 Commercial Devices at Three UK Urban Monitoring Sites. NERC EDS Centre for Environmental Data Analysis. 12 September 2024. Available online: https://catalogue.ceda.ac.uk/uuid/ae1df3ef736f4248927984b7aa079d2e/ (accessed on 1 June 2024).
53. Kok, G.; van Dijk, M.; Harris, P.; Vedurmudi, A. Modelling and determining correlations in sensor networks. In Proceedings of the XXIV IMEKO World Congress, Hamburg, Germany, 26–29 August 2024.
54. Takruri, M.; Challa, S. Drift aware wireless sensor networks. In Proceedings of the 10th International Conference on Information Fusion, Quebec, QC, Canada, 12 July 2007; pp. 1–7. [CrossRef]

55. Li, Z.; Wang, Y.; Yang, A.; Yang, H. Drift detection and calibration of sensor networks. In Proceedings of the International Conference on Wireless Communications and Signal Processing (WCSP), Nanjing, China, 15–17 October 2015; pp. 1–6. [CrossRef]
56. Munirathinam, S. Drift detection analytics for IoT sensors. *Procedia Comput. Sci.* **2021**, *180*, 903–912. [CrossRef]
57. *IEC 60584-1*; Thermocouples—Part 1: Emf Specifications and Tolerances. International Electrotechnical Commission: Geneva, Switzerland, 2013.
58. Martin, J.; Tritt, T.; Uher, C. High temperature Seebeck coefficient metrology. *J. Appl. Phys.* **2010**, *108*, 121101. [CrossRef]
59. Alcock, C.B.; Hooper, G.W. Thermodynamics of the gaseous oxides of the platinum-group metals. *Proc. R. Soc. London. Ser. A. Math. Phys. Sci.* **1960**, *254*, 551–561. [CrossRef]
60. Pearce, J.V. Optimising platinum-rhodium thermocouple wire compositions to minimize composition change due to evaporation of oxides. *Johns. Matthey Technol. Rev.* **2016**, *60*, 238–242. [CrossRef]
61. Pearce, J.V. A validated physical model of the thermoelectric drift of Pt-Rh thermocouples above 1200 °C. *Metrologia* **2020**, *57*, 025009. [CrossRef]
62. Gelman, A.; Carlin, J.B.; Stern, H.S.; Rubin, D.B. *Bayesian Data Analysis*, 2nd ed.; Chapman & Hall/CRC: Boca Raton, FL, USA, 2004.
63. Pearce, J. *Drift of Pt-Rh Thermocouples in Emf and in Temperature Terms at 1324 °C*; Zenodo: Genève, Switzerland, 2024. [CrossRef]